

Cosmic Rays on NICMOS: Results from Thermal Vacuum Data.

Daniela Calzetti and Chris Skinner
November 27, 1996

ABSTRACT

The analysis of NICMOS data obtained during the System Level Thermal Vacuum Test in August 1996 has yielded some information on the sensitivity of the NICMOS detectors to cosmic ray hits. The number of cosmic ray events (5σ detections) during the experiments was 0.067 events/Camera/sec in NIC3, 0.095 events/Camera/sec in NIC2, and 0.090 events/Camera/sec in NIC1, with an increase of 35-40% from NIC3 to NIC1/NIC2. We tentatively attribute this increase to secondary emission from the aluminum surrounding the detectors. The mean size of the 5σ cosmic ray hits is 1.65 pixels, with no significant variations from one Camera to the other. The number of affected pixels decreases for increasing DN values. If the on-orbit performance mirrors this situation, information in the affected pixels may be recovered in some cases with an appropriate use of the MULTI-ACCUM readout mode.

1. Introduction

The characterization of the sensitivity of the NICMOS detectors to cosmic ray (CR) hits is an important issue, since the results may determine observing strategies. As we will see in the next sections, extrapolations of the results from ground-based experiments to the on-orbit performance are bound to have large uncertainties, and only after launch will a clear determination of the CR-sensitivity of NICMOS be achieved. However, the results from the System Level Thermal Vacuum (SLTV) tests already suggest higher sensitivity to CR events than previously believed, and the consequences on observing strategies are briefly discussed in the Conclusion section.

2. The Analysis

The Data

Sets of 9 darks of 2089 seconds each were obtained during the SLTV tests in August 1996 for each of the 3 NICMOS detectors, using the ACCUM readout mode and NREAD=1. The data from each Camera were analyzed independently to check for systematics. The first image of each set showed higher average counts than the others by about 20 DN, and was discarded from the analysis. Therefore, 8 dark images were used for each Camera for a total of 16,712 seconds of dark exposure.

The Method

The detection of CR events was performed using the CRREJ routine in the STSDAS package of IRAF. The routine was developed to remove CR events in WFPC2 images and was improved during the analysis of the Hubble Deep Field images. CRREJ offers the possibility to iterate the rejection procedure using different thresholds at each iteration and to reject the pixels surrounding an identified CR event. The outputs from CRREJ are a “CR-free” image and mask images of the rejected pixels, in the same number as the input images.

For the specific case of the NICMOS darks, only the central $176 \times 176 \text{ pix}^2$ were analyzed in each frame, to avoid edge effects and the biases in the statistics introduced by the amplifier glow. The smallest rejection threshold was set to $T_{\text{CR}} = 5 \sigma$ in CRREJ, namely all the pixels which are above 5σ are flagged as affected by CR events. The radius of the region around an identified 5σ deviation and subject to further scrutiny was set to 1.5 pixels, and the rejection threshold for this area was set to two different values: $T_{\text{S}} = 5 \sigma$ and $T_{\text{S}} = 3 \sigma$. The two thresholds reject surrounding pixels as deviant as, and 1.67 times less deviant than, the primary “CR hit”.

Hot pixels in the NICMOS detectors should not appear in the masks of rejected pixels if there are not large variations in their intensity from one dark frame to the next. Indeed, an investigation of the “CR-free” images revealed that the detector’s hot pixels were still present in these images, and, therefore, were not counted as CR-affected pixels.

Since NICMOS has a small dark current (about $0.1 \text{ e}^-/\text{sec}$) and a large readout noise (about 30 e^-), the latter is the single most important parameter which determines the value of the rejection threshold. For the present analysis, a value of 30 e^- has been assumed for the readout noise in each Camera. As other analyses have shown, the readout noise is not expected to have large variations among the Cameras. It should be noted, however, that if the readout noise is 45 e^- , instead of 30 e^- , the number of CR-affected pixels decreases by about 13%. The gain was assumed to be 6 e^- .

Examples of the spatial distribution of the CR events onto the detectors are given in Figure 1 below.

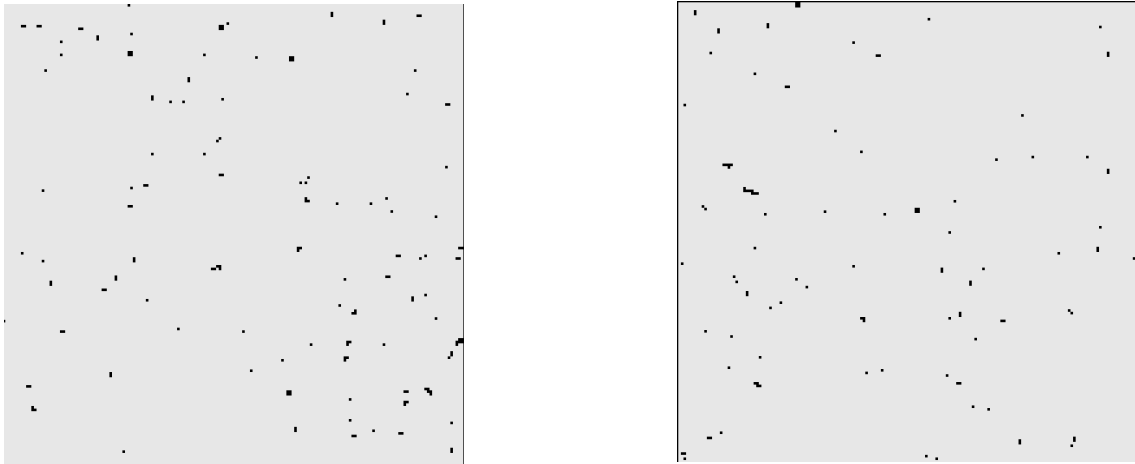


Figure 1: The distribution of CR events onto the NICMOS detectors is shown for one of the 2089 secs darks in NIC1 (left) and NIC3 (right), for the threshold $T_{CR}=5 \sigma$ and $T_S=5 \sigma$.

The energy distribution of the CR-affected pixels was determined by subtracting the “CR-free” image from the sum of the 8 darks, for the case $T_{CR}=5 \sigma$ and $T_S=5 \sigma$. The distribution of the energies of the affected pixels for Cameras NIC1 and NIC3 is shown in Figure 2 below.

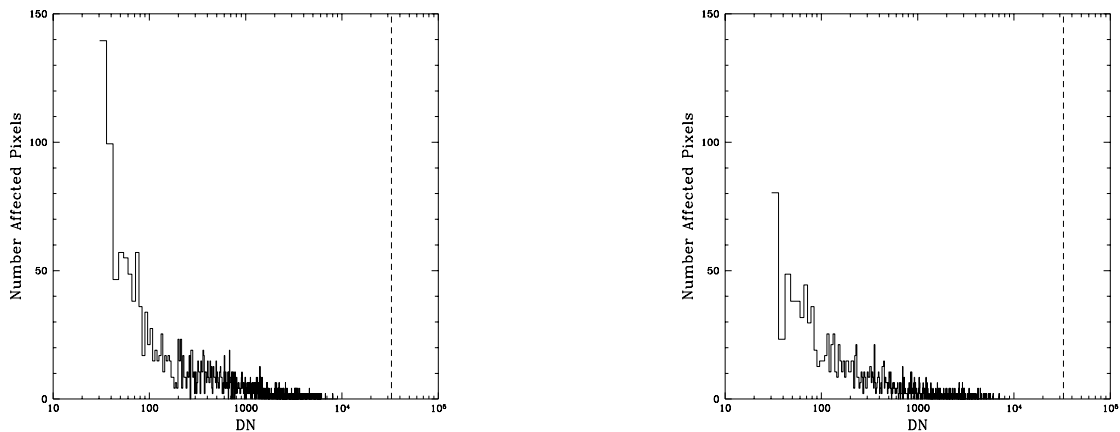


Figure 2: The energy distribution of the CR-affected pixels in NIC1 (left) and NIC3 (right), for the case $T_{CR}=5 \sigma$ and $T_S=5 \sigma$. The abscissa is expressed in DN, while the vertical axis shows the cumulative number of CR-affected pixels from the sum of 8 dark frames. The vertical dashed line marks the position of the saturation level (about 32700 DN). Most of the pixels are characterized by low energy values.

Results

The number of events detected, the mean size of the CR events, and the number of affected pixels, given in units of Camera and seconds, are reported in Table 1 below, for the two values of T_S considered. Although only the central portion of each frame was analyzed, the numbers reported are normalized to the entire area of each Camera.

Table 1: CR Event Statistics

Camera	Threshold	Number Events (#/Camera/sec)	Size of Events (pixels)	Affected Pixels (#/Camera/sec)
NIC1	$T_{CR}=5 \sigma, T_S=5 \sigma$	0.090	1.65	0.148
NIC1	$T_{CR}=5 \sigma, T_S=3 \sigma$	0.090	2.30	0.207
NIC2	$T_{CR}=5 \sigma, T_S=5 \sigma$	0.095	1.65	0.156
NIC2	$T_{CR}=5 \sigma, T_S=3 \sigma$	0.095	2.05	0.195
NIC3	$T_{CR}=5 \sigma, T_S=5 \sigma$	0.067	1.65	0.110
NIC3	$T_{CR}=5 \sigma, T_S=3 \sigma$	0.067	1.90	0.127

NIC1 and NIC2 show a larger number of affected pixels relative to NIC3, by about 40-50%, with some variation which depends on the chosen threshold. NIC1 is the innermost detector inside the NICMOS Cold Well; NIC2 occupies an intermediate position, while NIC3 is the closest to the surface of the dewar. The rough increase of affected pixels with depth of the detector inside the Cold Well could be interpreted as an effect of the secondary emission produced by the aluminum surrounding the detectors. This interpretation is supported by the number distribution of the CR-affected pixels (Figure 2), which is a decreasing function of the energy deposited in the pixel.

3. Conclusions: Extrapolation to On-Orbit Performance

The extrapolation of the results obtained from the SLTV data to on-orbit performance is haunted by our lack of knowledge of the responsivity of the NICMOS dewar+detectors to high altitude CRs (namely, protons) relatively to the ground-level CRs (mostly muons). The number of events could increase by factors ranging from roughly 10 to about 90 (the latter being the increase factor experienced by WFPC2).

For a ten-fold increase factor, there would be on average 2 affected pixels/camera/sec at the 5σ level, implying that 2% of the pixels in a detector are affected by CR hits every 660 seconds (this number decreases to 73 seconds for an increase factor of 90). However, most of the CRs will deposit a relatively small amount of energy onto the pixels, if the results from SLTV still hold on-orbit. The use of the MULTIACCUM readout mode should enable the recovery of the information in most of the 5σ -hit cases. The use of multiple non-destructive reads during an exposure, with each couple of readouts spaced by, say,

500 seconds or less, could be a viable solution to the handling of medium-energy CR events. In designing their observations, users should be aware that the amplifier glow increases with the number of non-destructive MULTIACCUM readouts, and that in many situations their exposures will be read-noise dominated. For instance, in the F160W filter, NIC1 is read-noise dominated for exposures up to 4000 seconds, NIC2 up to 1900 seconds, and NIC3 up to 330 seconds. The trade-off between these different factors should be considered when implementing observations.

More complex will be the handling of very low-energy CR-affected pixels: from Figure 2, it is clear that there is no obvious maximum to the energy distribution of the CR-affected pixels, and the peak of the distribution shifts towards lower energy values as the detection threshold T_{CR} decreases. For instance, the rate of rejected pixels is 0.47 /Camera/sec with $T_{CR}=3\sigma$ and $T_S=3\sigma$ in NIC1. Figure 3 shows the distribution of the rejected pixels for a 3σ threshold in one of NIC1 darks. The 3σ and lower CR events are hard to detect, since they get confused with the noise level of the image. If the on-orbit energy distribution of the CR-affected pixels reproduce the one observed during SLTV, and if we experience a large increase factor from ground to orbit, the net effect may be some loss in the sensitivity of the instrument.

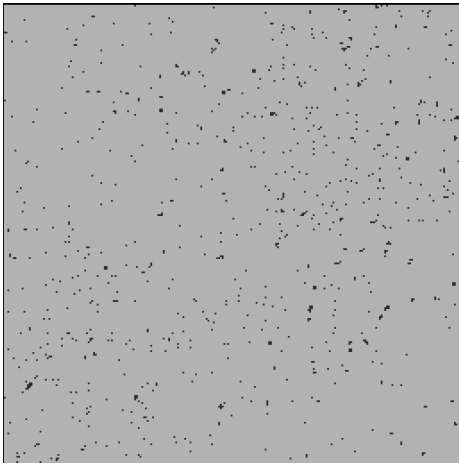


Figure 3: The rejected pixels in one of the NIC1 2089 secs darks, for thresholds $T_{CR}=3\sigma$ and $T_S=3\sigma$. On average, there are 988 rejected pixels. Under the assumption that each pixel is an independent realization of the same statistical distribution, we would expect only 177 rejected pixels/Camera. Therefore, CR hits contribute 82% of the rejected pixels in a 2089 sec ground-based dark.